ACS APPLIED MATERIALS & INTERFACES

Research Article

www.acsami.org

# Highly Sensitive Detection of Hormone Estradiol E2 Using Surface-Enhanced Raman Scattering Based Immunoassays for the Clinical Diagnosis of Precocious Puberty

Rui Wang,[†] Hyangah Chon,[†] Sangyeop Lee,[†] Ziyi Cheng,[†] Sung Hyun Hong,[‡] Young Ho Yoon,[‡] and Jaebum Choo*[,†]

[†]Department of Bionano Technology, Hanayng University, Ansan 426-791, South Korea

[‡]EOne Laboratories, Songdo 406-840, South Korea

Supporting Information

**ABSTRACT:** The hormone estradiol (17$\beta$-estradiol, E2) plays an important role in sexual development and serves as an important diagnostic biomarker of various clinical conditions. Particularly, the serum E2 concentration is very low (<10 pg/mL) in prepubertal girls. Accordingly, many efforts to develop a sensitive method of detection and quantification of E2 in human serum have been made. Nonetheless, current clinical detection methods are insufficient for accurate assessment of E2 at low concentrations (<10 pg/mL). Thus, there is an urgent need for new technologies with efficient and sensitive detection of E2 for use in routine clinical diagnostics. In this study, we introduce a new E2 assay technique using a surface-enhanced Raman scattering (SERS)-based detection method. The SERS-based assay was performed with 30 blood samples to assess its clinical feasibility, and the results were compared with data obtained using the ARCHITECT chemiluminescence immunoassay. Whereas the commercial assay system was unable to quantify serum levels of E2 lower than 10 pg/mL, the limit of detection of E2 using the novel SERS-based assay described in this study was 0.65 pg/mL. Thus, the proposed SERS-based assay has a strong potential to be a valuable tool in the early diagnosis of precocious puberty due to its excellent analytical sensitivity.

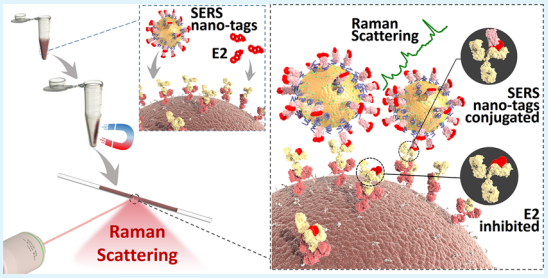


**KEYWORDS:** *surface-enhanced Raman scattering (SERS), 17 β-estradiol (E2), immunoassay, precocious puberty, clinical diagnosis*

## 1. INTRODUCTION

The hormone estradiol (17$\beta$-estradiol, E2) is a natural estrogen excreted by human and domestic animals and is produced primarily within the female ovaries or in the male testes.[1−3] E2 plays a vital role in various physiological processes, with a particular impact on reproductive and sexual function. In addition, E2 quantification is an indicator of a person's sexual maturation status and also helps doctors diagnose diseases associated with sex hormone imbalances.[4−6] Increased E2 production is largely responsible for breast development, genital growth, and changes in the distribution of body fat in pubescent girls. Thus, sensitive and specific assays for E2 are needed to track pubertal development and to better define the ranges of normal levels across childhood. The E2 concentration in serum is very low (<10 pg/mL) in prepubertal girls.[7,8] However, because of the absence of sensitive assays that can accurately quantify E2 at concentrations less than 10 pg/mL, many issues related to the role of E2 in pubertal development and growth remain unanswered. Thus, there is an urgent need to develop a highly sensitive method for the detection of E2 in human serum, especially in prepubertal children.

Many efforts have been employed to develop a sensitive detection method for the estimation of E2 in human serum including high-performance liquid chromatography−mass spectroscopy (HPLC-MS),[9−11] chemiluminescence immunoassay,[12] radioimmunoassay (RIA),[13] and enzyme-linked immunosorbent assay (ELISA).[14,15] Although mass spectrometry has a lower limit of detection of ∼10 pg/mL, it is associated with several analytical disadvantages such as long sample preparation steps and expensive instrumentation. For these reasons, mass spectrometry is not suitable for routine clinical applications. RIA allows for rapid, sensitive, and inexpensive screening of a large number of clinical samples, but the use of radioisotopes and scintillation fluids restricts its application for practical detection of E2 in human serum. Likewise, while ELISA has been widely used to screen E2, and various ELISA kits have been commercialized for quantitative identification of E2 in human serum, this approach does not meet the requirements for accurate assessment of E2 at low concentrations (<10 pg/mL). In ELISA assays, quantification of target molecule is achieved through observing enzyme-mediated color changes. However, discernible color change of antigen cannot be induced at low concentrations of target molecules, and the microplate reader fails to distinguish the color change. Because

Received: November 14, 2015
Accepted: April 12, 2016
Published: April 12, 2016






DOI: 10.1021/acsami.5b10996
ACS Appl. Mater. Interfaces 2016, 8, 10665−10672

of this detection limit, ELISA alone cannot suffice as an effective technique for sensitive detection of E2. Thus, there is an urgent need for new technologies that can achieve efficient and sensitive detection of E2 for use in routine clinical diagnostics.

Recently, surface-enhanced Raman scattering (SERS)-based immunoassay using functional nanomaterials has garnered much attention due to its high sensitivity.[16,17] To date, various kinds of biomarker proteins,[18−22] viruses,[23−25] and bacteria[26−29] have been successfully investigated using SERS-based assays. We believe that this SERS-based assay technique has a strong potential as a new emerging technology for the highly sensitive detection of E2. When reporter molecules are adsorbed onto the nanoparticle surface, their Raman signals are greatly increased at SERS-active sites well-known as "hot spots" due to electromagnetic and chemical enhancement effects. This enhancement has shown promises in overcoming low sensitivity problems inherent in E2 detection via ELISA. Furthermore, SERS-based immunoassays do not require any extraction or chromatography steps, amenable to the possibility of automated assay systems because the optical detection principle is similar to that of currently available fluorescence or luminescence immunoassay systems used in clinical laboratory settings. In addition, SERS-based immunoassays have the capability to meet the requirement for a low detection level (<1 pg/mL) of E2, an essential requirement for the diagnosis of precocious puberty. At present, the lowest detection level of E2 that can be measured with a commercially available chemiluminescence instrument is estimated to be >10 pg/mL.[30,31]

In the case of target antigen markers, the sandwich immunoassay platform has become popular for SERS-based immunoassays. Because the size of a protein molecule is relatively very large, it has multiple binding epitopes. In SERS-based sandwich immunoassays, capture antibodies are immobilized on the surfaces of magnetic beads, and detection antibodies are immobilized on the surface of SERS nanotags. Consequently, the protein antigen is sandwiched between the two antibodies, and the amount is quantified by monitoring the characteristic Raman peak intensity of SERS nanotags.[32−34] However, the small molecular size of E2 limits its binding epitope site. In the present work, therefore, we developed a SERS-based competitive immunoassay for highly sensitive E2 detection in clinical serum. To date, several SERS-based competitive immunoassay results also have been reported.[35−37] To the best of our knowledge, however, this is the first report of a competitive SERS-based E2 immunoassay of clinical serum. We believe that this approach will provide new insights into the early diagnosis of precocious puberty.

## 2. EXPERIMENTAL SECTION

**2.1. Materials.** Gold(III) chloride trihydrate ($HAuCl_4 \cdot 3H_2O$), 17 $\beta$-estradiol (E2), thiol-poly(ethylene glycol)-COOH (HS-PEG-COOH, MW ≈ 3500), and poly(ethylene glycol) methyl ether thiol (HS-PEG, MW = 2000) were purchased from Sigma-Aldrich (Missouri, U.S.A.). Malachite green isothiocyanate (MGITC), phosphate-buffered saline (PBS) (10× , pH 7.4), and carboxylic-activated magnetic beads (Dynabeads MyOne) were purchased from Invitrogen (Oregon, U.S.A.). Mouse antiestradiol monoclonal antibody (1 mg/mL) and goat antimouse IgG (2 mg/mL) were purchased from Abcam (Cambridge, U.K.). Estradiol-ovalbumin conjugate (E2-OVA) was purchased from Cusabio (Wuhan, China). Steroid-free human serum was purchased from Fitzgerald (Massachusetts, U.S.A.). The ultrapure water (18 MΩ·cm$^{-1}$) used in this work was prepared by a Milli-Q water purification system (Massachusetts, U.S.A.). All other reagents were from commercial sources, were of analytical reagent grade, and were used without further purification.

**2.2. Preparation of SERS nanotags.** Gold nanoparticles (Au NPs) were prepared using the citrate reduction method reported by Frens.[38] Briefly, 50 mL of $HAuCl_4$ (0.01% by weight) was heated to boiling, after which 0.5 mL of freshly prepared trisodium citrate solution (1% by weight) was added with vigorous stirring. Within a few seconds, the solution changed from colorless to deep red. The mixture was boiled for 15 min. Finally, the solution was cooled to room temperature with continuous stirring. The sizes of gold nanoparticles were characterized with dynamic light scattering (DLS) data and high-magnification transmission electron microscopy (TEM) images (Figure S1). According to our statistical analysis of TEM images and DLS data, the diameter of Au NPs is estimated to be 36.7 ± 5.5 nm.

SERS nanotags were prepared as described previously.[39,40] Briefly, Raman reporter MGITC solution (0.5 $\mu$L, $10^{-4}$ M) was added to 1.0 mL Au NPs (36.7 nm, 0.16 nM). Here, the concentration of Au NPs was calculated from the mean particle diameter (36.7 nm) and the weight of $HAuCl_4$ used in the preparation. Antibody conjugation was induced by the addition of heterofunctional linker HS-PEG-COOH into the solution. After shaking for 10 min, the HS-PEG-COOH (60 $\mu$L, 10 $\mu$M) was added dropwise to 1.0 mL of Au-MGITC solution with vigorous stirring. After 30 min of continuous stirring, the HS-PEG (120 $\mu$L, 10 $\mu$M) solution was added to the PEGylated Au-MGITC solution and reacted for 3 h. Subsequently, the PEGylated Au NPs were centrifuged to remove unbound PEG molecules (7200 rpm, which corresponds to 4810$g$ force, 10 min) and then resuspended in PBS (10 mM, pH 7.2).

To activate the −COOH groups on the surfaces of Au NPs, 1-ethyl-3-(3-dimethylaminopropyl)carbodiimide (EDC) (5 $\mu$L, 25 mM) and $N$-hydroxysulfosuccinimide (NHS) (5 $\mu$L, 25 mM) were mixed vigorously at 25 °C for 15 min. Excess EDC and NHS were then separated from the activated Au NPs through three rounds of centrifugation (7200 rpm, 10 min) and resuspended in PBS (10 mM, pH 7.2). The PEGylated Au NPs with activated carboxyl groups were then reacted with E2-OVA (2 $\mu$L, 1 mg/mL) at 25 °C for 2 h, and the reaction mixture was stored at 4 °C overnight. Excess E2-OVA was removed through three rounds of centrifugation (7200 rpm, 10 min) and resuspended in PBS (10 mM, pH 7.4). Figure S2 shows the (a) UV/vis spectra, (b) DLS distributions, and (c) SERS spectra of Au NPs with SERS nanotags.

**2.3. Preparation of antibody-conjugated magnetic beads.** To prepare the antibody-conjugated magnetic beads, 0.5 mL of 0.5 mg/mL carboxylic group-functionalized magnetic beads (MBs-COOH) were washed twice with 10 mM PBS (pH 7.2) and resuspended in PBS (10 mM, pH 7.2). The surfaces of the MBs were activated through incubation with EDC (5 $\mu$L, 0.1 M) and NHS (5 $\mu$L, 0.1 M) in an incubator shaker (500 rpm) at room temperature. Next, the MBs were separated by a magnet and washed twice with 10 mM PBS (pH 7.2). Then, the MBs were resuspended in 0.5 mL of 10 mM PBS (pH 7.2) and reacted with 2.5 $\mu$L of goat antimouse antibody (2 mg/mL) for ∼2 h with continuous shaking at room temperature. The immunomagnetic beads were then washed with PBS to remove nonspecifically bound antibodies and stored in 10 mM PBS (pH 7.4) at 4 °C.

**2.4. Instrumentation.** Raman measurements were obtained using a Renishaw inVia Raman microscope system (Renishaw, U.K.). A spectra physics He−Ne laser, operating at $\lambda$ = 632.8 nm, was used as the excitation source, with a power of ∼20 mW. The Rayleigh line was removed from the collected Raman scattering using a holographic notch filter located in the collection path. Raman scattering was collected using a charge-coupled device (CCD) camera. All spectra were calibrated to the 520 cm$^{-1}$ silicon line. An additional CCD camera was fitted to an optical microscope to obtain optical images. A 20× objective lens was used to focus a laser spot on the glass tube. All of the Raman spectra reported in this study were collected using a 1 s exposure time in the range of 630−1730 cm$^{-1}$. Baseline correction of Raman spectra was performed using software (WiRE 4.0, Renishaw,


DOI: 10.1021/acsami.5b10996
ACS Appl. Mater. Interfaces 2016, 8, 10665−10672

U.K.). Polynomial algorithm (polynomial order = 11) was used to all points in each spectrum, and the baseline has been corrected as zero. Quantitative analysis of E2 was performed by calculating the spectral Raman peak intensity of MGITC at 1613 $cm^{-1}$ to obtain their relative intensity values. A Cary 100 spectrometer was used to acquire UV/vis absorption spectra. DLS data were obtained using a Nano-ZS90 (Malvern), and TEM images were acquired using a JEOL JEM 2100F instrument at an accelerating voltage of 200 kV.

**2.5. Assays of clinical serum samples.** To assess the analytical reliability and clinical applicability of our proposed assay method, we carried out immunoassays on clinical samples. This clinical study was approved by the Institutional Review Board at EOne. A total of 30 blood samples from patients experiencing precocious puberty were collected from the EOne Clinical Laboratory, and all serum samples were stored at −80 °C until analyzed. Specifically, the clinical samples comprised 30 children (28 females and 2 males; age distribution 7−15) diagnosed with precocious puberty. The E2 level for each of the 30 clinical samples was determined using the SERS immunoassay protocol. In addition, each sample was assayed using a chemiluminescence assay system (ARCHITECT, Abbott Laboratories, U.S.A.) available in the EOne clinical laboratory. The assay procedures for the chemiluminescence assay were conducted according to the manufacturer's recommendations. Finally, the SERS results were compared with those measured with the chemiluminescence assay method.

**2.6. Statistical analysis of immunoassay results.** Passing-Boblok and Bland-Altman regression analyses[41,42] were carried out for all clinical data. Statistical analyses were used to estimate the analytical agreement and possible systematic bias between the two different methods. All statistical analyses were performed using MedCalc (Ostend, Belgium).

## 3. RESULTS AND DISCUSSION

**3.1. E2 assay protocols using SERS-based detection.** Figure 1 illustrates the SERS-based competitive immunoassay procedure for the quantification of E2. First, goat antimouse antibodies (secondary antibodies) are immobilized on the surfaces of magnetic beads (Figure 1a). Second, mouse anti-E2 monoclonal antibodies (primary antibodies) bind to secondary antibodies through an antibody−antibody interaction (Figure 1b). When free target E2 and E2-OVA-conjugated SERS nanotags are mixed with magnetic beads, they react competitively with anti-E2 antibodies on the surfaces of the magnetic beads. After the formation of immunocomplexes, their Raman signals can be measured and analyzed for E2 quantification (Figure 1c). In this assay, the observed Raman signal intensity decreased with increasing level of E2 in solution.

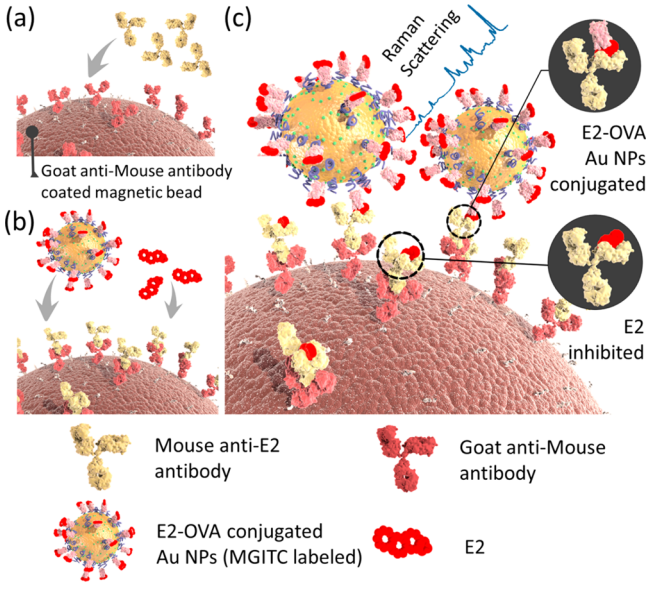


**Figure 1.** Schematic illustration of the SERS-based competitive immunoassay for quantification of E2. (a) Secondary antibody immobilization; (b) primary antibody immobilization by the antibody−antibody interaction; (c) target E2 and E2-conjugated SERS nanotags competitively react with anti-E2 antibody on magnetic beads.

Figure 2 shows a schematic of the procedure for the SERS-based competitive immunoassay using Au NPs and magnetic beads. Here, the Au NPs and magnetic beads were employed as SERS nanotags and separation agents, respectively. First, 25 μL of secondary antibody-conjugated magnetic beads and 25 μL of anti-E2 were mixed together and incubated for 90 min at room temperature. Second, 25 μL of E2 standard solution (concentrations: 0, 0.1, 0.5, 1, 3, 5, 7, 10, 30, 50, 100, 300, 500, and 1000 pg/mL in steroid-free human serum) and 50 μL of E2-OVA-conjugated SERS nanotags were mixed together and allowed to undergo a competitive immunoreaction, after which they were incubated for 2 h at room temperature. Third, the magnetic immunocomplexes were isolated via a magnetic bar on the wall of the microtube, and the remaining unbound SERS nanotags were washed with a micropipette three times. Finally, the immunocomplexes were redispersed in 25 μL of PBS (10 mM, pH 7.4), and the immunocomplexes in suspensions were transferred to a capillary tube for Raman measurements. Here, MGITC was used as a Raman reporter molecule, and its vibrational assignment is listed in Table S1. The strongest Raman peak intensity centered at 1613 $cm^{-1}$ was used for quantitative evaluation of E2. Using this SERS-based competitive assay, highly sensitive and reproducible detection of E2 standard solutions could be achieved at a single excitation wavelength.

**3.2. Optimization of immunoassay parameters.** To determine the optimal assay conditions, we investigated several experimental parameters including the concentration of anti-E2, the incubation time for the interaction between primary and secondary antibodies, the concentration of E2-OVA for maximum conjugation onto the surface of Au NPs, the volume ratio between magnetic beads and SERS nanotags, and the incubation time for formation of immunocomplexes.

First, different concentrations of anti-E2 (0.15, 0.20, 0.25, 0.30, 0.35, 0.40, 0.45, 0.50, 0.55, and 0.60 μg/mL) were assayed against solutions containing 1.0 ng/mL of E2 to identify the optimal concentration of anti-E2. Specifically, 25 μL of magnetic beads with different concentrations of anti-E2 were incubated with 25 μL of 1.0 ng/mL E2. After incubation for 2 h, followed by washing with PBS-Tween 20 buffer (10 mM, pH 7.4), 250 μL of E2-OVA-immobilized Au NPs (SERS nanotags) was added and incubated for 2 h. After washing and dispersing the SERS nanotags in 25 μL of PBS (10 mM, pH 7.4), the Raman signals of immunocomplexes were measured and analyzed. As shown in Figure S3a, at the low concentration of anti-E2, the binding sites of anti-E2 were fully occupied with E2. As a result, no binding sites remained on the surfaces of magnetic beads for SERS nanotags; thus, the Raman signal intensity did not show any significant change with increasing concentration of anti-E2. On the other hand, as the anti-E2 concentration increased, more binding sites became available, and the results of this experiment indicated that the E2 binding efficiency was maximized at an anti-E2 concentration of 0.55 μg/mL. As the concentration of anti-E2 exceeded this concentration, however, excess binding sites were occupied


DOI: 10.1021/acsami.5b10996
ACS Appl. Mater. Interfaces 2016, 8, 10665−10672

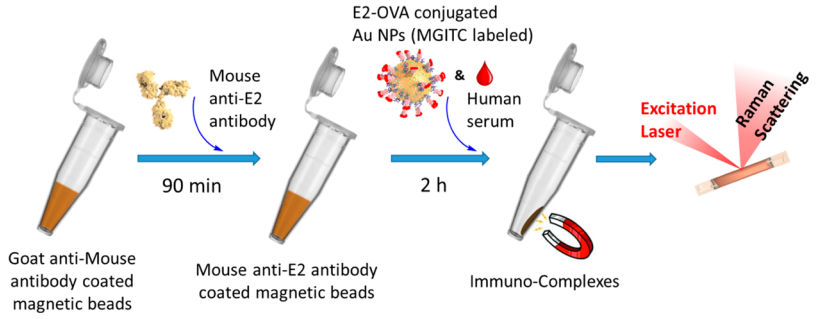


**Figure 2.** Schematic of the procedure for the SERS-based competitive immunoassay using SERS nanotags and magnetic beads.

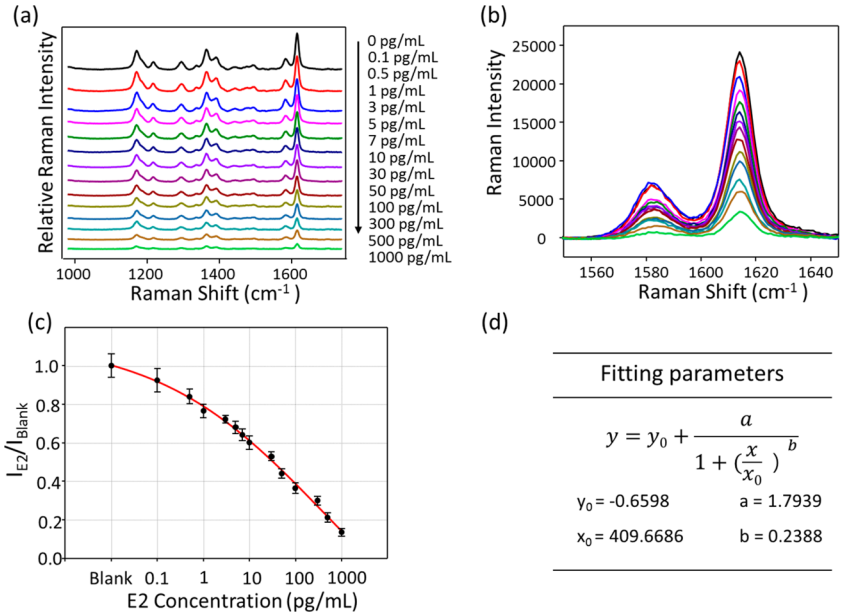


**Figure 3.** (a) SERS spectra for decreasing concentrations of E2; (b) SERS intensity variation at 1613 $cm^{-1}$; (c) corresponding calibration line of the SERS signal intensity at 1613 $cm^{-1}$ as a function of the logarithm of the concentration of E2; (d) four-parameter logistic function for the fitting line. Error bars indicate the standard deviation of five measurements.

by SERS nanotags. As a result, a significant increase in Raman signal was observed for concentrations of 0.6 $\mu$g/mL. For these reasons, the optimum anti-E2 concentration was ~0.55 $\mu$g/mL.

We next investigated the optimal incubation time for the interaction between anti-E2 (primary antibody) and goat antimouse IgG (secondary antibody). Specifically, we measured the Raman signal intensities for a range of incubation times (15, 30, 45, 60, 75, 90, 105, 120, and 135 min). As shown in Figure S3b, the Raman signal intensity reached a maximum threshold at 90 min, which was selected as the optimal incubation time for subsequent experiments.

Third, the optimum concentration of E2-OVA conjugated onto Au NPs (Figure S3c) was also investigated. In this set of experiments, different concentrations of E2-OVA (0.5, 1.0, 1.5, 2.0, 2.5, 3.0, 3.5, and 4.0 $\mu$g/mL) were used, and a maximum Raman signal intensity was obtained at a concentration of 2.0 $\mu$g/mL. Finally, we investigated the optimal volume ratio and incubation time among magnetic beads, SERS nanotags, and E2 (Figures S3d and S3e). According to our experimental data, the optimal volume ratio and incubation time were determined to be 1:2:1 and 2 h, respectively.

**3.3. Assessment of SERS-based competitive immunoassay.** Figure 3a shows the Raman spectra of magnetic immunocomplexes for various concentrations of E2. Here, different concentrations of E2 were spiked into commercially available steroid-free human serum solution. Baseline corrections for all spectra should be performed to obtain their relative intensity values. Raman spectra before and after the baseline correction are compared with each other in Figure S4. Blank Raman peak intensity signal was obtained in the absence of E2 and was used as a control. The relative Raman intensity of MGITC at 1613 $cm^{-1}$ was also monitored to quantify E2 concentration as shown in Figure 3b. The concentration of E2 varied from 0 to 1000 pg/mL, and the Raman peak of MGITC centered at 1613 $cm^{-1}$ was used for quantitative evaluation of E2. Conversely, as the concentration of E2 increased, more E2 molecules were able to form immunocomplexes with magnetic beads, resulting in fewer SERS nanotags attached to the surfaces of the magnetic beads. Consequently, the Raman signal intensity was concomitantly decreased with increasing E2 concentration. On the basis of the ratio of peak intensities ($I_{E2}/I_{blank}$), the calibration curve for the quantitative evaluation of E2 was constructed. It is possible to perform quantitative analysis of E2 marker in clinical serum using this calibration line. The corresponding calibration curve from the Raman intensity variations at 1613 $cm^{-1}$ is shown in Figure 3c. The fitting curve was determined from the four-parameter logistic function in Figure 3d. Raman intensity gradually decreased in a logarithmic


DOI: 10.1021/acsami.5b10996
ACS Appl. Mater. Interfaces 2016, 8, 10665−10672

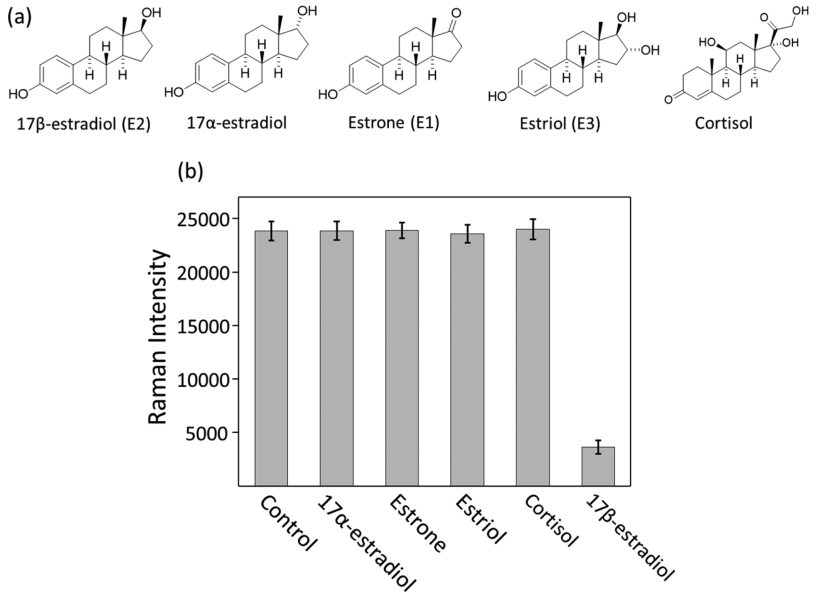


**Figure 4.** Selectivity test of the SERS-based assay for (a) E2 and four different E2 analogues and (b) their corresponding SERS intensities at 1613 $cm^{-1}$. Error bars indicate the standard deviations of five measurements.

manner with increasing concentration of E2 and exhibited a good response in the range of 0.1−1000 pg/mL. The error bars in the figure indicate the standard deviation of five measurements.

To assess the detection sensitivity and potential clinical applicability of our proposed SERS-based competitive immunoassay, we compared it with a commercially available E2 ELISA kit (Abnova). For this comparison, a total of 10 different concentrations of E2 were prepared. For concentrations of the E2 solution including 0, 0.1, 0.5, 1.0, 5.0, 10, 30, 100, 300, and 1000 pg/mL, the standard solutions in the kit were used, while E2 solutions with a concentration lower than 10 pg/mL were prepared by diluting the standard solution. We performed ELISA assays with all concentrations according to the manufacturer's protocol. As shown in Figure S5, the assay data achieved by our SERS-based assay method (Figure S5b) were in good agreement with those obtained from the commercial ELISA kit (Figure S5a) for higher concentrations of E2 (>5 pg/mL). On the other hand, there was a reduced correspondence between ELISA and SERS assay data in the low-concentration regime. As shown in Figure S5a, it was difficult to quantify E2 using ELISA for concentrations less than 5 pg/mL. However, the SERS-based assay results were much more consistent in the low-concentration range (0−5 pg/mL) than were those achieved by the commercial ELISA kit, suggesting that the SERS-based immunoassay technique allows for more sensitive quantification of E2 than does ELISA.

Importantly, the limit of detection (LOD) for the SERS-based immunoassay, estimated as three standard deviations from the background, was 0.83 pg/mL, while that of ELISA was ∼2.3 pg/mL. In the commercial E2 ELISA kit, however, a different kind of antibody was used and its corresponding different binding affinity might influence the LOD. To confirm the low LOD result in our SERS-based assay, ELISA assays using a commercially available anti-E2 antibody (Abcam, U.K.) were performed. Here, the same antibody that was used for our SERS-based assays was utilized. According to our experimental results, the LOD determined from the ELISA assay using the same antibody as with the SERS-based assay was estimated to be 123 pg/mL. This value is ∼3 orders of magnitude less sensitive than that (0.83 pg/mL) of the corresponding SERS-based method using the same antibody. Consequently, it was concluded that the low LOD in the SERS-based assay is not caused by different binding affinities of antibodies.

To evaluate the selectivity of the SERS-based assay for E2, we next investigated its ability to detect four similar compounds, namely, 17$\alpha$-estradiol, estrone (E1), estriol (E3), and cortisol (Figure 4a). Consistent with our results described above, the SERS intensity was greatly decreased for E2, while no obvious changes in intensity changes were observed for any of the other four compounds, as shown in Figure 4b. This observation indicated that the antibody-conjugated magnetic beads only capture E2, and thus the SERS-based assay technique described in this study is useful for selective E2 quantification.

**3.4. Evaluation of SERS-based immunoassay for clinical samples.** To assess the clinical applicability of our proposed assay technique, we carried out SERS-based immunoassays on clinical samples, and the results were compared with chemiluminescence assay data, as shown in Table 1. Before performing the immunoassay on the clinical samples, E2 calibration curves for both chemiluminescence and SERS-based assays were generated using E2 calibrators of known concentration. In the SERS-based assay, the Raman intensity at 1613 $cm^{-1}$ was monitored, and the E2 concentration was calculated using a calibration fitting curve in Figure 3c.

Passing-Boblok regression analysis was applied to estimate the agreement and possible systematic bias between the two different analytical methods. Figure 5a shows scatter plots (purple points) and associated regressions (blue line) of the data, which revealed good agreement between the two analytical methods, as the 95% confidence intervals (CIs) for the intercept and slope included 0 and 1, respectively. The 95% CI values satisfied both conditions, indicating that all values were within the clinically acceptable range and also that the SERS assay data were clinically valid. Here, 11 clinical samples (sample nos. 1−11 in Table 1) were not included in statistical


DOI: 10.1021/acsami.5b10996
ACS Appl. Mater. Interfaces 2016, 8, 10665−10672

**Table 1. Comparison of Quantitative Results Determined by Chemiluminescence and SERS-Based Immunoassays for E2 Clinical Samples (28 Females and 2 Males; Age Distribution 8−15)**

| sample no. | gender | age (years) | chemiluminescence assay[a] (pg/mL) | SERS-based assay (pg/mL) | standard deviation (SERS-based assay) |
|---|---|---|---|---|---|
| 1 | F | 8 | <10 | 5.37 | ±1.24 |
| 2 | F | 8 | <10 | 4.59 | ±0.91 |
| 3 | F | 8 | <10 | 2.22 | ±0.62 |
| 4 | F | 8 | <10 | 7.66 | ±1.45 |
| 5 | F | 8 | <10 | 2.66 | ±0.72 |
| 6 | F | 9 | <10 | 9.43 | ±1.25 |
| 7 | F | 10 | <10 | 9.02 | ±1.33 |
| 8 | F | 7 | <10 | 11.7 | ±0.65 |
| 9 | F | 8 | <10 | 8.52 | ±1.14 |
| 10 | F | 10 | <10 | 10.3 | ±1.35 |
| 11 | F | 9 | <10 | 3.87 | ±0.72 |
| 12 | F | 8 | 15 | 23.6 | ±0.45 |
| 13 | F | 8 | 18 | 22.9 | ±2.15 |
| 14 | F | 8 | 14 | 19.9 | ±2.05 |
| 15 | F | 8 | 17 | 26.9 | ±2.43 |
| 16 | F | 9 | 12 | 17.6 | ±1.85 |
| 17 | F | 9 | 17 | 22.8 | ±1.31 |
| 18 | M | 10 | 11 | 16.3 | ±2.25 |
| 19 | F | 8 | 16 | 24.0 | ±2.94 |
| 20 | F | 10 | 19 | 26.3 | ±0.99 |
| 21 | F | 8 | 15 | 18.7 | ±1.18 |
| 22 | F | 8 | 12 | 14.8 | ±1.37 |
| 23 | F | 9 | 13 | 18.8 | ±1.39 |
| 24 | F | 13 | 39 | 45.6 | ±2.57 |
| 25 | F | 10 | 27 | 32.3 | ±2.73 |
| 26 | F | 12 | 56 | 56.3 | ±2.79 |
| 27 | F | 13 | 29 | 34.9 | ±2.05 |
| 28 | M | 15 | 22 | 28.9 | ±0.87 |
| 29 | F | 10 | 89 | 98.5 | ±2.78 |
| 30 | F | 9 | 26 | 30.4 | ±1.26 |

[a]Difficult to quantify E2 in serum for assay concentrations less than 10 pg/mL.

analysis because the commercially available chemiluminescence-detection instrument cannot meet the requirements for accurate assessment of E2 at low concentrations, <10 pg/mL.

In addition, the precision profile corresponding to the functional sensitivity of SERS-based immunoassay is displayed in Figure 5b. Here, functional sensitivity (limit of quantification, LOQ) is defined as the lowest concentration that can be measured with a coefficient variation (CV) less than or equal to 20%.[43] Mean and % CV were calculated from 30 clinical samples with three replicates. The calculated % CVs were plotted against the corresponding means for all clinical sera. A reciprocal curve was fitted through the data, and the functional sensitivity was estimated as the concentration corresponding to the 20% CV level of the curve. In this calculation, the functional sensitivity of our SERS-based assay is determined to be 4.78 pg/mL. In other words, it is possible to carry out an accurate quantitative analysis for assay concentrations higher than 5.0 pg/mL (over gray region). According to the commercial instrument instruction, however, the functional sensitivity of chemiluminescence is 25.0 pg/mL. On the basis of our experimental results, we concluded that the SERS-based assay can be successfully applied for highly sensitive quantification of serum E2, especially at low concentrations (<10 pg/mL).

## 4. CONCLUSIONS

In the present study, we demonstrated a novel SERS-based competitive immunoassay technique for highly sensitive quantification of E2. In this assay, target E2 and E2-OVA-conjugated SERS nanotags reacted competitively with anti-E2 antibodies immobilized on the surfaces of magnetic beads. The amount of E2 marker was successfully measured by monitoring the characteristic Raman peak intensity of SERS nanotags. To determine the feasibility of the proposed assay for clinical application, assay conditions including antibody concentration, incubation time, and volume ratio between magnetic beads and SERS nanotags were carefully optimized.

To assess the detection sensitivity of our proposed SERS-based competitive assay, the assay results were compared with those obtained by a commercially available E2 ELISA kit (Abnova). While it was difficult to quantify E2 using ELISA for concentrations less than 5 pg/mL, the SERS-based assay results were more consistent in the low-concentration range (0−5 pg/mL), demonstrating that the SERS-based immunoassay technique allows for more sensitive quantification of E2 than does ELISA. In addition, the SERS-based assay described in this study exhibited excellent selectivity for E2 when tested against four similar compounds.

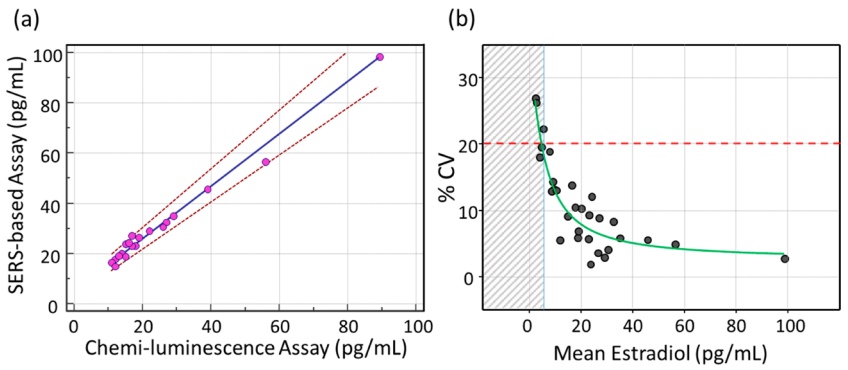


**Figure 5.** (a) Passing-Boblok regression plot for the determination of the bias and compatibility between chemiluminescence and SERS. The solid blue line is the regression line, and the two dotted lines show the 95% CI range. (b) Precision profile corresponding to the functional sensitivity of SERS-based immunoassay. % CVs were plotted against the corresponding means for 30 clinical sera.


DOI: 10.1021/acsami.5b10996
ACS Appl. Mater. Interfaces 2016, 8, 10665−10672

SERS-based assays were performed for 30 blood samples to assess their clinical feasibility. The results were then compared with the data obtained by the ARCHITECT chemiluminescence assay system. Using this commercial assay system, however, it was impossible to quantify E2 in serum for assay concentrations lower than 10 pg/mL. Accordingly, the early diagnosis of precocious puberty is difficult in many cases because of the poor analytical sensitivity of E2 ELISA. In the case of our SERS-based assay, however, the LOD for E2 was estimated to be ~0.65 pg/mL. Thus, the SERS-based assay described in this study has strong potential as a valuable tool for early diagnosis of precocious puberty.

## ■ ASSOCIATED CONTENT

### Supporting Information

The Supporting Information is available free of charge on the ACS Publications website at DOI: 10.1021/acsami.5b10996.

TEM image and dynamic light scattering data of Au NPs, characterization of SERS nanotags, optimization of immunoassay parameters, baseline correction process for acquired Raman spectra, comparison of the assay data between chemiluminescence and SERS, and table summarizing vibrational assignment of MGITC in its SERS spectrum (PDF)

## ■ AUTHOR INFORMATION

### Corresponding Author

* E-mail: jbchoo@hanayng.ac.kr.

### Notes

The authors declare no competing financial interest.

## ■ ACKNOWLEDGMENTS

The National Research Foundation of Korea supported this work through Grant nos. 2008-0061891 and 2009-00426. The Nano Material Technology Development Program also supported this work, through the National Research Foundation of Korea, funded by the Ministry of Science, ICT & Future Planning (2012M3A7B4035288).

## ■ REFERENCES

(1) Ström, A.; Hartman, J.; Foster, J. S.; Kietz, S.; Wimalasena, J.; Gustafsson, J. Estrogen Receptor $\beta$ Inhibits 17 $\beta$-Estradiol-Stimulated Proliferation of the Breast Cancer Cell Line T47D. *Proc. Natl. Acad. Sci. U. S. A.* **2004**, *101*, 1566−1571.

(2) Tai, S. S.-C.; Welch, M. J. Development and Evaluation of a Reference Measurement Procedure for the Determination of Estradiol-17$\beta$ in Human Serum Using Isotope-Dilution Liquid Chromatography−Tandem Mass Spectrometry. *Anal. Chem.* **2005**, *77*, 6359−6363.

(3) Struble, R. G.; Nathan, B. P.; Cady, C.; Cheng, X. Y.; McAsey, M. Estradiol Regulation of Astroglia and Apolipoprotein E: An Important Role in Neuronal Regeneration. *Exp. Gerontol.* **2007**, *42*, 54−63.

(4) Stricker, R.; Eberhart, R.; Chevailler, M. C.; Quinn, F. A.; Bischof, P.; Stricker, R. Establishment of Detailed Reference Values for Luteinizing Hormone, Follicle Stimulating Hormone, Estradiol, and Progesterone During Different Phases of the Menstrual Cycle on the Abbott ARCHITECT® Analyzer. *Clin. Chem. Lab. Med.* **2006**, *44* (7), 883−887.

(5) Elliott, K. J.; Cable, N. T.; Reilly, T.; Diver, M. J. Effect of Menstrual Cycle Phase on the Concentration of Bioavailable 17-$\beta$ Oestradiol and Testosterone and Muscle Strength. *Clin. Sci.* **2003**, *105*, 663−669.

(6) Wu, C. H.; Motohashi, T.; Abdel-Rahman, H. A.; Flickinger, G. L.; Mikhail, G. Free and Protein-Bound Plasma Estradiol-17$\beta$ During the Menstrual Cycle. *J. Clin. Endocrinol. Metab.* **1976**, *43* (2), 436−445.

(7) Bay, K.; Andersson, A. M.; Skakkebaek, N. E. Estradiol Levels in Prepubertal Boys and Girls–Analytical Challenges. *Int. J. Androl.* **2004**, *27*, 266−273.

(8) Fossa, S. D.; Klepp, O.; Barth, E.; Aakvaag, A.; Kaalhus, O. Endocrinological Studies in Patients with Metastatic Malignant Testicular Germ Cell Tumours. *Int. J. Androl.* **1980**, *3*, 487−501.

(9) Stopforth, A.; Burger, B. V.; Crouch, A. M.; Sandra, P. The Analysis of Estrone and 17$\beta$-Estradiol by Stir Bar Sorptive Extraction−Thermal Desorption−Gas Chromatography/mass Spectrometry: Application to Urine Samples after Oral Administration of Conjugated Equine Estrogens. *J. Chromatogr. B: Anal. Technol. Biomed. Life Sci.* **2007**, *856*, 156−164.

(10) Thienpont, L. M.; Verhaeghe, P. G.; Van Brussel, K. A.; De Leenheer, A. P. Estradiol-17$\beta$ Quantified in Serum by Isotope Dilution-gas Chromatography-mass Spectrometry: Reversed-phase C18 High-performance Liquid Chromatography Compared with Immuno-affinity Chromatography for Sample Pretreatment. *Clin. Chem.* **1988**, *34*, 2066−2069.

(11) Stanczyk, F. Z.; Clarke, N. J. Advantages and Challenges of Mass Spectrometry Assays for Steroid Hormones. *J. Steroid Biochem. Mol. Biol.* **2010**, *121*, 491−495.

(12) Xin, T. B.; Chen, H.; Lin, Z.; Liang, S. X.; Lin, J. M. A Secondary Antibody Format Chemiluminescence Immunoassay for the Determination of Estradiol in Human Serum. *Talanta* **2010**, *82*, 1472−1477.

(13) Shirtcliff, E. A.; Granger, D. A.; Schwartz, E. B.; Curran, M. J.; Booth, A.; Overman, W. H. Assessing Estradiol in Biobehavioral Studies Using Saliva and Blood Spots: Simple Radioimmunoassay Protocols, Reliability, and Comparative Validity. *Horm. Behav.* **2000**, *38* (2), 137−147.

(14) Schneider, C.; Schöler, H. F.; Schneider, R. J. A Novel Enzyme-linked Immunosorbent Assay for Ethynylestradiol Using a Long-chain Biotinylated EE2 Derivative. *Steroids* **2004**, *69*, 245−253.

(15) Valentini, F.; Compagnone, D.; Gentili, A.; Palleschi, G. An Electrochemical ELISA Procedure for the Screening of 17$\beta$-Estradiol in Urban Waste Waters. *Analyst* **2002**, *127*, 1333−1337.

(16) Grubisha, D. S.; Lipert, R. J.; Park, H. Y.; Driskell, J.; Porter, M. D. Femtomolar Detection of Prostate-Specific Antigen: An Immunoassay Based on Surface-Enhanced Raman Scattering and Immunogold Labels. *Anal. Chem.* **2003**, *75*, 5936−5943.

(17) He, L. L.; Rodda, T.; Haynes, C. L.; Deschaines, T.; Strother, T.; Diez-Gonzalez, F.; Labuza, T. P. Detection of a Foreign Protein in Milk Using Surface-Enhanced Raman Spectroscopy Coupled with Antibody-Modified Silver Dendrites. *Anal. Chem.* **2011**, *83*, 1510−1513.

(18) Chon, H.; Lee, S.; Yoon, S. Y.; Chang, S. I.; Lim, D. W.; Choo, J. Simultaneous Immunoassay for the Detection of Two Lung Cancer Markers Using Functionalized SERS Nanoprobes. *Chem. Commun.* **2011**, *47*, 12515−12517.

(19) Chon, H.; Lee, S.; Son, S. W.; Oh, C. H.; Choo, J. Highly Sensitive Immunoassay of Lung Cancer Marker Carcinoembryonic Antigen Using Surface-Enhanced Raman Scattering of Hollow Gold Nanospheres. *Anal. Chem.* **2009**, *81*, 3029−3034.

(20) Lee, M.; Lee, S.; Lee, J. H.; Lim, H.; Seong, G. H.; Lee, E. K.; Chang, S.-I.; Oh, C. H.; Choo, J. Highly Reproducible Immunoassay of Cancer Markers on a Gold-patterned Microarray Chip Using Surface-Enhanced Raman Scattering Imaging. *Biosens. Bioelectron.* **2011**, *26*, 2135−2141.

(21) Chon, H.; Lee, S.; Yoon, S.-Y.; Lee, E. K.; Chang, S.-I.; Choo, J. SERS-based Competitive Immunoassay of Troponin I and CK-MB Markers for Early Diagnosis of Acute Myocardial Infarction. *Chem. Commun.* **2014**, *50*, 1058−1060.

(22) Campbell, F. M.; Ingram, A.; Monaghan, P.; Cooper, J.; Sattar, N.; Eckersall, P. D.; Graham, D. SERRS Immunoassay for Quantitative Human CRP Analysis. *Analyst* **2008**, *133*, 1355−1357.

(23) Paul, A. M.; Fan, Z.; Sinha, S. S.; Shi, Y.; Le, L.; Bai, F.; Ray, P. C. Bioconjugated Gold Nanoparticle Based SERS Probe for Ultra-



DOI: 10.1021/acsami.5b10996
ACS Appl. Mater. Interfaces 2016, 8, 10665−10672

sensitive Identification of Mosquito-Borne Viruses Using Raman Fingerprinting. *J. Phys. Chem. C* **2015**, *119*, 23669−23675.
(24) Han, Z.; Liu, H.; Wang, B.; Weng, S.; Yang, L.; Liu, J. Three-Dimensional Surface-Enhanced Raman Scattering Hotspots in Spherical Colloidal Superstructure for Identification and Detection of Drugs in Human Urine. *Anal. Chem.* **2015**, *87*, 4821−4828.
(25) Shao, F.; Lu, Z.; Liu, C.; Han, H.; Chen, K.; Li, W.; He, Q.; Peng, H.; Chen, J. Hierarchical Nanogaps within Bioscaffold Arrays as a High-Performance SERS Substrate for Animal Virus Biosensing. *ACS Appl. Mater. Interfaces* **2014**, *6*, 6281−6289.
(26) Wang, J.; Wu, X.; Wang, C.; Shao, N.; Dong, P.; Xiao, R.; Wang, S. Magnetically Assisted Surface-Enhanced Raman Spectroscopy for the Detection of Staphylococcus aureus Based on Aptamer Recognition. *ACS Appl. Mater. Interfaces* **2015**, *7*, 20919−20929.
(27) Kumar, S.; Lodhi, D. K.; Goel, P.; Neeti; Mishra, P.; Singh, J. P. A Facile Method for Fabrication of Buckled PDMS Silver Nanorod Arrays as Active 3D SERS Cages for Bacterial Sensing. *Chem. Commun.* **2015**, *51*, 12411−12414.
(28) Zhou, H.; Yang, D.; Ivleva, N. P.; Mircescu, N. E.; Schubert, S.; Niessner, R.; Wieser, A.; Haisch, C. Label-Free in Situ Discrimination of Live and Dead Bacteria by Surface-Enhanced Raman Scattering. *Anal. Chem.* **2015**, *87*, 6553−6561.
(29) Costas, C.; López-Puente, V.; Bodelón, G.; González-Bello, C.; Pérez-Juste, J.; Pastoriza-Santos, I.; Liz-Marzán, L. M. Using Surface Enhanced Raman Scattering to Analyze the Interactions of Protein Receptors with Bacterial Quorum Sensing Modulators. *ACS Nano* **2015**, *9*, 5567−5576.
(30) Rollins, G. "A Call for Better Estradiol Measurement". *Clin. Lab. News* **2013**, May.
(31) Stanczyk, F. Z.; Jurow, J.; Hsing, A. W. Limitations of Direct Immunoassays for Measuring Circulating Estradiol Levels in Postmenopausal Women and Men in Epidemiologic Studies. *Cancer Epidemiol., Biomarkers Prev.* **2010**, *19*, 903−906.
(32) Porter, M. D.; Lipert, R. J.; Siperko, L. M.; Wang, G.; Narayanan, R. SERS as a Bioassay Platform: Fundamentals, Design, and Applications. *Chem. Soc. Rev.* **2008**, *37*, 1001−1011.
(33) Li, J. F.; Huang, Y. F.; Ding, Y.; Yang, Z. L.; Li, S. B.; Zhou, X. S.; Fan, F. R.; Zhang, W.; Zhou, Z. Y.; Wu, D. Y.; Ren, B.; Wang, Z. L.; Tian, Z. Q. Shell-isolated Nanoparticle-Enhanced Raman Spectroscopy. *Nature* **2010**, *464*, 392−395.
(34) Kim, I.; Junejo, I.; Lee, M.; Lee, S.; Lee, E. K.; Chang, S.-I.; Choo, J. SERS-based Multiple Biomarker Detection Using a Gold-patterned Microarray Chip. *J. Mol. Struct.* **2012**, *1023*, 197−203.
(35) Zhu, G. C.; Hu, Y. J.; Gao, J.; Zhong, L. Highly Sensitive Detection of Clenbuterol using Competitive Surface-enhanced Raman Scattering Immunoassay. *Anal. Chim. Acta* **2011**, *697*, 61−66.
(36) Liu, J. Z.; Hu, Y. J.; Zhu, G. C.; Zhou, X. M.; Jia, L.; Zhang, L. Highly Sensitive Detection of Zearalenone in Feed Samples Using Competitive Surface-Enhanced Raman Scattering Immunoassay. *J. Agric. Food Chem.* **2014**, *62*, 8325−8332.
(37) Gao, R.; Ko, J.; Cha, K.; Jeon, J. H.; Rhie, G.; Choi, J.; deMello, A. J.; Choo, J. Fast and Sensitive Detection of an Anthrax Biomarker Using SERS-based Solenoid Microfluidic Sensor. *Biosens. Bioelectron.* **2015**, *72*, 230−236.
(38) Frens, G. Controlled Nucleation for the Regulation of the Particle Size in Monodisperse Gold Suspensions. *Nature, Phys. Sci.* **1973**, *241*, 20−22.
(39) Maiti, K. K.; Dinish, U. S.; Fu, C. Y.; Lee, J. J.; Soh, K. S.; Yun, S. W.; Bhuvaneswari, R.; Olivo, M.; Chang, Y. T. Development of Biocompatible SERS Nanotag with Increased Stability by Chemisorption of Reporter Molecule for in Vivo Cancer Detection. *Biosens. Bioelectron.* **2010**, *26*, 398−403.
(40) Qian, X.; Peng, X. H.; Ansari, D. O.; Yin-Goen, Q.; Chen, G. Z.; Shin, D. M.; Yang, L.; Young, A. N.; Wang, M. D.; Nie, S. In Vivo Tumor Targeting and Spectroscopic Detection with Surface-Enhanced Raman Nanoparticle Tags. *Nat. Biotechnol.* **2008**, *26*, 83−90.
(41) Passing, H.; Bablok, W. A New Biometrical Procedure for Testing the Equality of Measurements from Two Different Analytical Methods. *J. Clin. Chem. Clin. Biochem.* **1983**, *21*, 709−720.
(42) Bland, J. M.; Altman, D. G. Statistical Methods for Assessing Agreement between Two Methods of Clinical Measurement. *Lancet* **1986**, *327*, 307−310.
(43) Lawson, G. M. Defining Limit of Detection and Limit of Quantification as Applied to Drug of Abuse Testing: Striving for a Concensus. *Clin. Chem.* **1994**, *40*, 1218−1219.


DOI: 10.1021/acsami.5b10996
*ACS Appl. Mater. Interfaces* 2016, 8, 10665−10672